J. Phys. B: At. Mol. Opt. Phys. **24** (1991) 4215-4230. Printed in the UK

State-selective double capture in collisions of bare ions with helium atoms at low energies: I. Total cross sections

Z Chen, R Shingal and C D Lin

Department of Physics, Kansas State University, Manhattan, KS 66506, USA

Received 19 October 1990, in final form 17 April 1991

Abstract. Double capture cross sections to individual doubly excited states for collisions between bare ions of carbon and oxygen with helium atoms in the energy range of a few keV amu^{-1} are calculated. By adopting an independent-electron approximation, the capture probability to each doubly excited state is calculated in terms of products of single capture amplitudes properly weighted with configuration-interaction coefficients, while the single capture amplitudes are calculated using a two-centre atomic orbital close-coupling expansion method with an extended basis set. The resulting cross sections are compared with recent results from high-resolution Auger electron measurements to assess the validity of the independent-electron approximation as well as the mechanism of double capture. It is shown that there is qualitative agreement between the present results and experiments.

1. Introduction

In recent years double electron capture between a multiply charged ion and a many-electron target atom or molecule has been studied in many laboratories. In earlier studies, the energy gain spectroscopy method has been used to show that double capture processes are important in these collisions. The resolution of these earlier experiments is incapable of identifying individual doubly excited states populated in the collision. With the advent of high-resolution Auger electron spectroscopy and the high-intensity multiply-charged ion beams available from the ECR sources in different countries, a large amount of experimental data where absolute or relative cross sections to individual doubly excited states have been reported have emerged. These experiments show that, in general, doubly excited states are selectively populated.

Despite the experimental activities in this area and the progress of ion–atom collision theory for single-electron processes made in the last decade, there have been very few theoretical calculations for such two-electron collision processes. This is partly due to the complexity of the processes involved. Consider, for example, the collision of a beam of bare oxygen ions at a few keV amu^{-1} energy from the ECR source with helium atoms. Experiments have shown that double capture results in populating mostly doubly excited states of the $3l3l'$ and $3l4l'$ manifolds and smaller populations of the higher $3lnl'$ ($n \geq 5$) manifolds (Mack *et al* 1989, Moretto-Capelle *et al* 1989). These doubly excited states, most of which autoionize to the $n=2$ level of the hydrogenic oxygen ion, are observed by electron spectroscopy. Experimentalists usually measured the electron yield at a given ejection angle of the electron, from which the populations of individual doubly excited states were deduced. We will show in the following paper that this procedure is questionable when the doubly excited states populated are strongly overlapped.

0953-4075/91/194215+16$03.50

From the theoretical viewpoint, one of the many difficulties for such a collision process is the large number of states populated. Within the $3l3l'$ manifold (to be abbreviated as the (3, 3) manifold), there are already 11 singlet states. For the (3, 4) manifold, there are 28 singlet states. At such low collision energies, models based on the close-coupling method are obviously the most suitable. In principle, the close-coupling expansion based on the two-electron atomic or molecular orbitals (see e.g. Fritsch and Lin 1986, Kimura *et al* 1983, Harel and Jouin 1990) can be formulated to solve the time-dependent Schrödinger equation, but the actual implementation for such a collision system is clearly very complicated. Besides the 39 states in the (3, 3) and (3, 4) manifolds mentioned above, one must also include single capture to the $n=3$ and $n=4$ states of the hydrogenic oxygen ion which are the dominant channels populated. Thus one easily needs more than 100 basis functions (counting the different magnetic states) in the calculation. Such a large calculation has not been attempted. A two-electron calculation with a moderate size of basis functions has recently been carried out by Harel and Jouin (1990) for double capture in N^{7+}–He collisions.

In view of such practical difficulties, we recently proposed an independent-electron model which was applied to study double capture to individual (2, 2) doubly excited states in $He^+ + He$ collisions (Jain *et al* 1989). A similar model was first adopted by Salin *et al* as quoted in Zourous *et al* (1987). In this paper we apply the same model to double capture (*a*) to the (2, 3) and (3, 3) doubly excited states in C^{6+}–He collisions; and (*b*) to the (3, 3) and (3, 4) doubly excited states in O^{8+}–He collisions. These calculations are then compared with recent experiments from different groups to assess the validity of the independent-electron approximation.

The next section gives a brief summary of the theoretical model used. Application and analysis of the present calculations are given in section 3 where we also compare the theoretical results with experiments. A word of caution is needed at this point. Since most of the experimental state-selective capture cross sections were *derived*, under a number of assumptions, from the Auger electron spectra measured at one or a few angles, we believe that one needs to treat these derived experimental cross sections carefully.

In the accompanying paper (Chen and Lin 1991) the calculated state-selective capture *amplitudes* are combined with the Auger decay amplitudes to predict the ejected-electron spectra. We stress that theoretical models should calculate the ejected electron spectra which are then compared with experimental measurements directly. We will also discuss circumstances where unambiguous state-selective double capture cross sections can be deduced from experimental electron spectra. A short summary of this paper is given in section 4.

2. Theory

Consider the collision of a bare ion of charge Z with a helium target atom, the time-dependent Schrödinger equation is

$$\left[-\tfrac{1}{2}\nabla_1^2-\tfrac{1}{2}\nabla_2^2-\frac{2}{r_{1a}}-\frac{2}{r_{2a}}+\frac{1}{r_{12}}-\frac{Z}{r_{1b}}-\frac{Z}{r_{2b}}-\mathrm{i}\frac{\partial}{\partial t}\right]\Psi(\boldsymbol{r}_1,\boldsymbol{r}_2,t)=0 \tag{1}$$

where a and b refer to the helium and the bare ion nucleus, respectively. One version of the independent-electron model is to replace the $1/r_{12}$ term with a screening potential. With such a replacement, the resulting equation becomes separable for electrons 1 and

2, and the two-electron wavefunction can be written as

$$\Psi(\boldsymbol{r}_1, \boldsymbol{r}_2, t) = \phi(\boldsymbol{r}_1, t)\phi(\boldsymbol{r}_2, t) \tag{2}$$

where the one-electron wavefunction satisfies

$$\left(-\tfrac{1}{2}\nabla_1^2 + V(r_{1a}) - \frac{Z}{r_{1b}} - \mathrm{i}\frac{\partial}{\partial t} \right) \phi(\boldsymbol{r}_1, t) = 0 \tag{3}$$

and where the 'model potential' V includes the screening between the two electrons. In our calculation $V(r)$ was chosen (see Shingal 1988) such that the ground and singly excited state energies of He are well reproduced.

In our calculation, equation (3) is solved by the close-coupling approach by expanding $\phi(\boldsymbol{r}, t)$ using atomic orbitals about the two collision centres. For such a one-electron system, there is no difficulty in including up to 50–70 basis functions for each impact parameter. The one-electron wavefunction centred at the projectile after the collision (at impact parameter b) can be expressed as

$$\phi(\boldsymbol{r}_1, t \to \infty) = \sum_{nlm} a_{nlm}(b) u_{nlm}(\boldsymbol{r}_1) \tag{4}$$

where $u_{nlm}(r_1)$ is a hydrogenic wavefunction of charge Z. According to this model, the two-electron wavefunction on the projectile as $t \to \infty$ is

$$\Psi(\boldsymbol{r}_1, \boldsymbol{r}_2, t \to \infty) = \sum_{nlm} \sum_{n'l'm'} a_{nlm}(b) a_{n'l'm'}(b) u_{nlm}(\boldsymbol{r}_1) u_{n'l'm'}(\boldsymbol{r}_2). \tag{5}$$

To extract the capture amplitude we project $\Psi(\boldsymbol{r}_1, \boldsymbol{r}_2, t \to \infty)$ into each doubly excited state on the projectile. In our calculations, these wavefunctions are expressed in terms of linear combinations of products of hydrogenic wavefunctions. Thus the important configuration interactions in the wavefunctions of the doubly excited states are included. After this projection, the double capture probability amplitude to each state at each impact parameter b is obtained. The cross sections are calculated by integrating the probabilities over impact parameters.

In the model above, the procedure is not variational and the results depend on the model potential $V(r)$ chosen for the one-electron calculation. For one-electron processes such as single capture and single ionization, $V(r)$ is chosen such that the binding energies of the ground state and the first few excited states of helium are in agreement with experimental values. Such a potential (Shingal 1988) was used for the first electron in the present calculation. However, if such a potential is also used for the second electron, the energy needed to remove both electrons is $2 \times 0.9 = 1.8$ au, while the actual experimental value is 2.9 au. Within the independent-electron model, we account for the change of screening by adopting a different model potential for the second electron. In fact, we chose $V(r_a) = -2/r_a$ for the second electron so that the total ionization energy to remove the second electron is correct. This procedure also ensures that the inelastic energy loss (or gain) between the initial and final states of the two-electron system is correct. This can also be interpreted as assuming that the second electron is completely relaxed after the first electron has been removed, or that the second electron is captured from the smaller distances where the screening by the other electron can be neglected. After the two wavefunctions ϕ_1 and ϕ_2 from each model have been calculated, the two-electron wavefunction is constructed as

$$\Psi(\boldsymbol{r}_1, \boldsymbol{r}_2, t) = [\phi_1(\boldsymbol{r}_1)\phi_2(\boldsymbol{r}_2) + \phi_2(\boldsymbol{r}_1)\phi_1(\boldsymbol{r}_2)]/\sqrt{2}. \tag{6}$$

Since the initial state is a singlet, only singlet state wavefunctions are considered. We emphasize that this procedure preserves unitarity despite the fact that two separate calculations have been carried out. To obtain the transition amplitude to a specific state, (6) is then projected into the well defined atomic wavefunction of that state. Since electron correlation is accounted for in the final atomic wavefunctions, this model neglects most of the electron–electron interaction only during the collision. One expects that this procedure would be most applicable for collisions with multiply charged ions, but this speculation has to be checked by comparing with actual experimental results.

3. Results and discussion

3.1. $C^{6+}+He$

3.1.1. The correlation diagram. This collision system, together with $O^{6+}+He$, has been studied by many experimental groups for both the one-electron and two-electron transition processes using ions from ECR sources (see Stolterfoht *et al* 1990 and references therein). To obtain a qualitative estimate of the important states populated in such a collision, we show in figure 1 the schematic *diabatic* correlation diagram. Each potential curve $U_i(R)$ is given by $U_i(R)=Z_pZ_t/R+E_i$, where Z_p and Z_t are the net charges of the two ions in the separated-atom (SA) limit and E_i is the corresponding electronic energy, also in the SA limit. For single capture channels, the energy E_i can be easily calculated using Bohr's formula. For double capture channels, the energy E_i can be estimated from the double Rydberg formula for intrashell states and from the quantum defect theory for intershell states (Lin 1989). In this work we used the energies actually calculated from the CI code. In figure 1 the energy scale has been shifted such that the potential curve for the entrance $C^{6+}+He$ channel is a horizontal line. The slope of each potential curve is determined by the repulsive potential Z_pZ_t/R. Curves representing double capture channels are steeper than those representing single capture

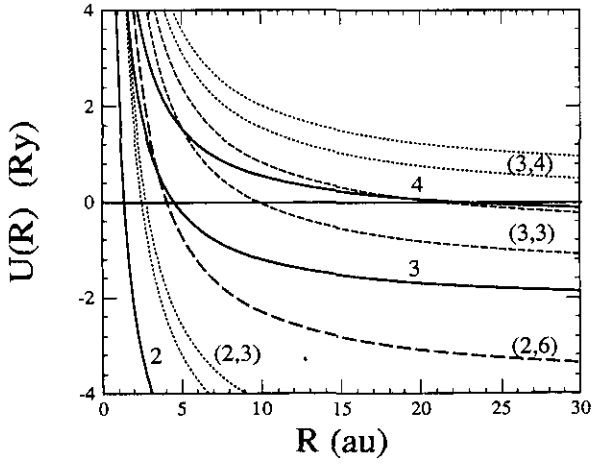

Figure 1. Schematic diabatic potential curves for the dominant single and double capture channels for the $C^{6+}+He$ system. The absolute energy scale has been shifted so that the entrance channel is represented by a horizontal $U(R)=0$ line. The doubly excited state channels are represented by a band, bound by the lowest and highest states, for each (n, n') manifold.

channels. Since there are many channels within each (n, n') manifold of doubly excited states, only the two curves representing the lowest and highest energies within each manifold are given. If one of the electrons is in a high-n Rydberg state such as the doubly excited states in the (2, 6) manifold, the width of each manifold is narrow and is not visible in the diagram. Table 1 shows the values of the crossing radius for single capture to $n = 2$, 3 and 4 states and double capture to the $(2, n)$ $(n = 3\text{-}6)$ and the (3, 3) manifolds. Note that the $(3, n)$ $(n \geqslant 4)$ manifolds do not cross the entrance channel directly.

The correlation diagram shown in figure 1 differs from the one shown in Stolterfoht *et al* (1990) where doubly excited states were designated and the energies were calculated using the independent-particle approximation.

Table 1. Crossing radii (R_c) of the entrance channel with the dominant single and double capture channels for $C^{6+} + He$.

Single capture	$n = 2$	$n = 3$	$n = 4$		
R_c (au)	2.1	5.0	21.0		
Double capture	(2, 3)	(2, 4)	(2, 5)	(2, 6)	(3, 3)
R_c (au)	2.5	3.3	3.8	4.1	9.9–21.0

3.1.2. Single capture channels. From table 1 one notices that the crossings for single capture to $n = 4$, 3 and 2 states occur at $R = 21$, 5, and 2.1 au, respectively. The crossing at $R = 21$ au is too far out and can be treated as diabatic while the crossing at $R \approx 2$ au is in the 'molecular' region where the diabatic representation is not useful. The crossing at $R = 5$ for single capture to $n = 3$ states is expected to be the most favourable. This is easily confirmed by an estimate based on the classical over-barrier model, or from the results of close-coupling calculations. The later methods have been applied to calculate single electron capture cross sections for the C^{6+}, O^{6+}–He systems by expanding the time-dependent two-electron wavefunction in terms of atomic basis functions (Fritsch and Lin 1986) or molecular basis orbitals (Kimura and Olson 1984, Shimakura *et al* 1987). In these calculations the number of basis functions included is limited and the weak doubly excited state channels were not included. In the present calculation we need to solve only the one-electron close coupling equation. A much larger basis set was used, including the $n = 2$, 3, and 4 capture channels as well as a few pseudostates on both the projectile and the target centre. For each impact parameter, two calculations with different electron–target interactions were carried out. In the first one a model potential $V(r)$ (Shingal 1988) was used for He. In the second calculation a Coulomb potential $-2/r$ was used for He^+. The charge of the projectile in the two calculations remains the same.

In the present calculation, the single capture cross sections are not derived from the one-electron wavefunction. Instead, they are derived by projecting (6) into single capture final states where one of the electrons is on the excited states of the projectile and the other is the 1s state of He^+. This differs from many calculations based on the independent-particle approximation where the transitions involving the second electron are not considered. The cross sections thus calculated for single capture to $n = 4$, 3, and 2 are 1.30, 11.0 and 0.47, in units of 10^{-16} cm^2. These results, as shown in table 2, are in good agreement with the calculations of Fritsch and Lin (1986) and with the

Table 2. Comparison of cross sections for single capture to $n = 2$, 3 and 4 states and double capture to doubly excited states in the $2l3l'$, $3l3l'$, $3l4l'$ manifolds for 60 keV $C^{6+} + He$ collisions. The cross sections are in units of 10^{-17} cm^2.

	Experiment	Theory
$n = 2$		4.7[b]
$n = 3$	80[a]	110.0[b] 126[d]
$n = 4$	16[a]	13.0[b] 13.8[d]
$2l3l'$	10.6 ± 0.3[c]	8.2[b]
$3l3l'$	2.4 ± 0.2[c]	2.5[b]
$3l4l'$	1.32 ± 0.1[c]	5.4[b]

[a] Results for $O^{6+} + He$ from Dijkkamp *et al* (1985).
[b] Present calculations.
[c] Stolterfoht *et al* (1990).
[d] Fritsch and Lin (1986).

measurements of Dijkkamp *et al* (1985). They are also in agreement with the data of Liu *et al* (1989). There is no substantial disagreement between the theoretical and experimental results and one can conclude that the single-electron capture process for this system is well understood.

3.1.3. Double capture to each manifold of doubly excited states. There have been no theoretical studies of state-selective double capture cross sections for this system. Estimates based on the extended overbarrier model (Niehaus 1986) have been made. Experimental electron spectra resulting from double capture to $2lnl'$ ($n \geq 3$) and $3lnl'$ ($n \geq 3$) doubly excited states have been observed at different angles (Stolterfoht *et al* 1990, Mack *et al* 1989, Sakaue *et al* 1989, 1990). Only Stolterfoht *et al* (1990) have attempted to deduce absolute double capture cross sections. To get such information from the experimental electron spectra measured at a particular angle, a number of assumptions about the formation and the decay of doubly excited states must be made. The Auger electron distributions are often assumed to be isotropic for each state, and an average fluorescence yield was used for each manifold. Absolute experimental cross sections for double capture to $2lnl'$ and $3lnl'$ ($n \geq 3$) doubly excited states for 60 keV $C^{6+} + He$ collisions thus obtained have been reported recently by Stolterfoht *et al* (1990). We show in table 2 their results and the comparison with the calculated values for double capture to the $2l3l'$, $3l3l'$ and $3l4l'$ manifolds. In general, the agreement between the calculated and experimental results is surprisingly good, particularly if one recognizes that the cross section for double capture to the largest double capture manifold ($2l3l'$) is less than 10% of the cross section for single capture to the $n = 3$ states. For the weaker $3l3l'$ and $3l4l'$ manifolds, the ratios are only a few per cent. The theoretical results for the $3l4l'$ manifold is much larger than the experimental result. We mention that there are 28 states within this manifold and the large cross section is a result of adding up small cross sections from many channels.

3.1.4. Calculation of state-selective double capture cross sections. As discussed in section 2, two separate calculations were made to obtain single electron capture amplitudes which were then combined to calculate probabilities for double capture to individual doubly excited states. The two calculations represent the two successive steps in the

double capture process employed in the present independent-electron approximation. In the first calculation, the electron in helium has a binding energy of −0.9 au, while in the second calculation the binding energy is −2.0 au.

To get a qualitative understanding of the doubly excited states populated, it is helpful to examine the single capture probabilities from each calculation. Because of the shift of binding energies of the target in the two models, the dominant states and the region of impact parameters where each state is populated are different in the two calculations. In figures 2(*a*) and (2*b*) we show $b\,P_i(b)$ for the dominant channels. For electron capture from neutral helium (figure 2(*a*)) the states populated are mostly 3p and 3d, with b in the range of 2-5 au. Capture from the second electron (figure 2(*b*)) is also mostly to 3p and 3d states, but at impact parameters less than 2 au.

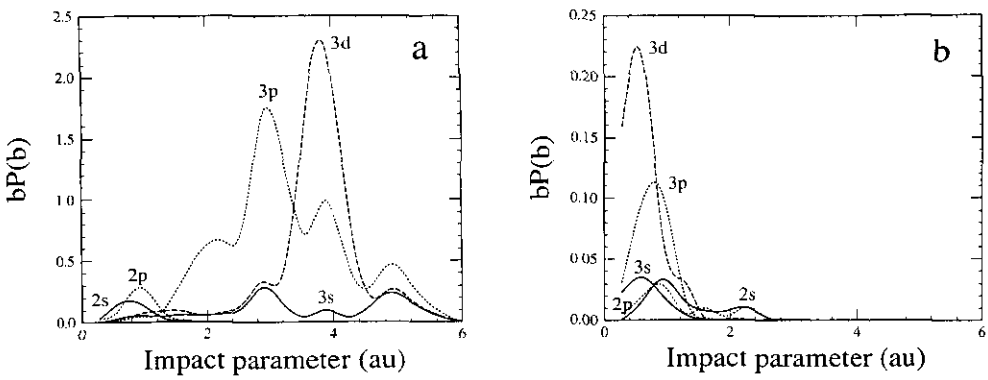

Figure 2. Impact parameter weighted probabilities for single capture to each *nl* state. (*a*) Single capture probabilities by C^{6+} from neutral He; (*b*) single capture probabilities by C^{6+} from He^+. The collision energy is 67 keV.

According to the independent-electron model, the probability for populating each doubly excited state is *roughly* equal to the product of these single electron capture probabilities. By inspection, it is clear that the impact parameter region where 3p and 3d probabilities are large in the two calculations do not overlap very well, thus resulting in small double capture probabilities to the (3, 3) manifold. On the other hand, the region where the probabilities for $n=2$ states are large in one calculation overlaps well with the region where the probabilities for $n=3$ states are large in the other calculation, thus the $2l3l'$ states are predominantly populated.

We have combined single electron capture amplitudes to calculate double capture cross sections to individual doubly excited states in the (2, 3) manifold. The results for collision energy at 67 keV are shown in figure 3(*a*). This is the energy used in the measurement of Sakaue *et al* (1989, 1990), which is close to the energy of 60 keV in the measurement of Stolterfoht *et al* (1990). In figure 3(*a*) each state is labelled by the $(K, T)^A$ quantum numbers (Lin 1986). It appears that high-L states are populated. We cannot compare figure 3(*a*) with the experimental electron spectra directly since the branching ratio for the Auger decay of each doubly excited state and the angular distributions of the Auger electrons have to be considered. This consideration is addressed in the accompanying paper (Chen and Lin 1991).

Unlike photon and electron impact excitation to doubly excited states from the ground state of an atom where there is evidence that only $A=+1$ states are populated,

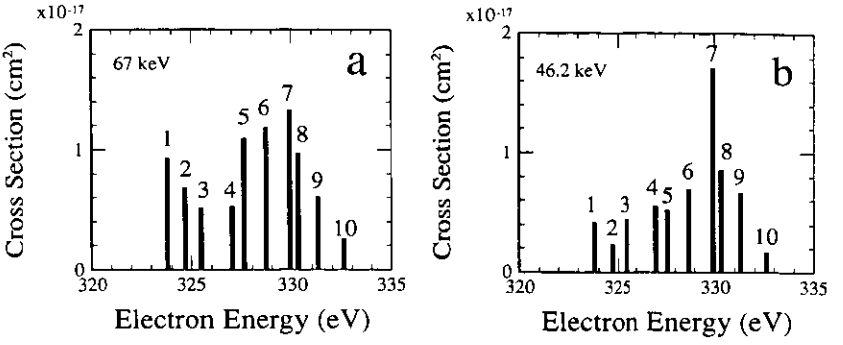

Figure 3. Calculated double capture cross sections for $C^{6+}+He \Rightarrow C^{4+}(2l3l')+He^{2+}$ at (*a*) 67 keV and (*b*) 46.2 keV. The numbered states are: 1, $(1,0)^-$ $^1P^o$; 2, $(1,0)^+$ $^1S^e$; 3, $(0,1)^-$ $^1P^e$; 4, $(0,1)^-$ $^1D^o$; 5, $(1,0)^+$ $^1D^e$; 6, $(0,1)^+$ $^1P^o$; 7, $(0,1)^0$ $^1D^e$; 8, $(1,0)^0$ $^1F^o$; 9, $(-1,0)^0$ $^1P^o$; 10, $(-1,0)^+$ $^1S^e$.

double capture to doubly excited states does not have any apparent selection rules in the quantum number A. One notes that electron–electron interaction (or correlation) plays the major role for forming doubly excited states in electron and photon impact, but for double capture the electron–electron interaction may play only a minor role, as exemplified in the present model where double capture is considered as two successive single capture events in a single collision.

The double capture cross sections are relatively sensitive to the collision energy. In figure 3(*b*) we show the calculated cross sections for the collision at 46.2 keV. At this lower energy, the cross sections for all the states within the (2, 3) manifold are less evenly distributed. The electron spectra from Sakaue *et al* (1989, 1990) agree with this result.

The calculated total capture cross sections to the (2, 3) manifold at 46.2 and 67 keV are 6.2×10^{-17} cm^2 and 8.0×10^{-17} cm^2, respectively. We note that in general the total cross section within a manifold is less sensitive to the collision energy than the state-selective cross sections. This is reflected also in the energy dependence of the total single capture cross sections σ_n for a given n which are less sensitive than the individual σ_{nl} (Fritsch and Lin, 1986).

We have also calculated the total double capture cross sections to each doubly excited state in the (3, 3) manifold. The state-selective cross sections for the two collision energies of 67 and 46.2 keV are shown in figures 4(*a*) and 4(*b*), respectively. We note that the relative strengths of the doubly excited states populated are quite different at the two energies. The calculated total cross sections are 1.82×10^{-17} cm^2 and 2.47×10^{-17} cm^2 at 46.2 and 67 keV energies for the (3, 3) manifold, respectively. These cross sections are about a factor of three less than the (2, 3) manifold.

3.1.5. Mechanism of populating doubly excited states. In this subsection we consider the mechanism for double capture to doubly excited states in $C^{6+}+He$ collisions with the aim of addressing the validity of the independent-electron approximation. There have been many experiments carried out for the isocharged O^{6+}–He collision system and many controversies in the interpretation of the mechanism of double capture (see for example, Stolterfoht *et al* 1990 and references therein). In this respect, the angle-resolved energy gain measurement of Roncin *et al* (1989) for the latter system can be used to establish the range of internuclear distances where a specific manifold of

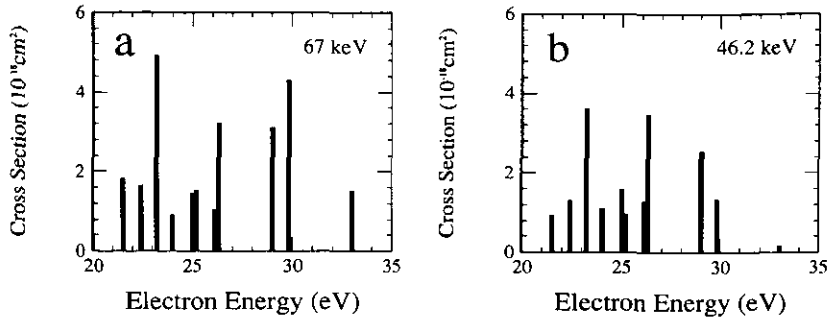

Figure 4. Calculated double capture cross sections for $C^{6+}+He \Rightarrow C^{4+}$ $(3l3l')+He^{2+}$ at (*a*) 67 and (*b*) 46.2 keV. The states beginning with the lowest one are: 1, (2, 0) $^1S^e$; 2, (2, 0) $^1D^e$; 3, (1, 1) $^1P^o$; 4, (1, 1) $^1D^o$; 5, (0, 2) $^1D^e$; 6, (0, 0) $^1s^e$; 7, (2, 0) $^1G^e$; 8, (1, 1) $^1F^o$; 9, (0, 0) $^1D^e$; 10, (−1, 1) $^1P^o$; 11, (+2, 0) $^1S^e$. All the intrashell states have $A = +1$ and the A quantum number is not labelled.

doubly excited states is populated. The latter system has also been studied by many experimental groups using electron spectroscopy with the Auger electrons measured at different angles. Two groups of electrons were identified. (*a*) Those from the Coster-Kronig transitions of the $2lnl'$ ($n \geq 6$) states. Such transitions are not energetically possible for $2lnl'$ states if $n \leq 5$. (*b*) Those from the L-Auger decay of $3lnl'$ ($n \geq 3$) states. The relative intensities of the two groups of electrons differ significantly from different laboratories. Such discrepancies have been discussed by Bordenave-Montesquieu *et al* (1987, 1989) and most recently by Stolterfoht *et al* (1990) where the discrepancies were attributed to instrumental problems associated with the measurement of low-energy Coster-Kronig and L-Auger electrons.

It has been suggested by Stolterfoht *et al* (1986, 1990 and references therein) in a series of papers that the non-equivalent configurations such as $2p6l$ states in O^{6+}–He collisions are populated by a correlated one-step process, while the equivalent configurations such as $3l3l'$ are populated by uncorrelated two-step processes. On the other hand, Boudjema *et al* (1989) have suggested that the one-step process is also responsible for the formation of $3l3l'$ states.

In the absence of actual calculations based on the molecular orbital picture, the conjecture of the collision mechanism is based on the diabatic correlation diagram (figure 1). In terms of such diabatic curves, a one-step process is defined to be a transition which occurs as a result of the crossing between the entrance channel with another diabatic curve. An obvious example of this is the single capture to the $n = 3$ states at $R = 5.1$ au. The probability for capture to the 3p and 3d states is significant only when the internuclear distance is less than about 5.1 au. This is illustrated by the calculated probability distributions for the 3p and 3d states (see figure 2(*a*)). The small $n = 4$ states are populated *not* at the crossing at $R = 22$ au, but at small impact parameters where the couplings among the diabatic curves are strong. Similarly, single capture to the $n = 2$ states occurs at small values of R.

We next address the mechanism of double capture to doubly excited states. We first discuss whether the (3, 3) manifold can be populated by the one-step mechanism since it has a crossing with the entrance channel in the range of 9–21 au. Experimental data from Roncin *et al* (1989) (their figure 3) indicate that the (3, 3) manifold is populated at larger scattering angles than the single capture to the $n = 3$ states. Thus the one-step (or a single crossing) mechanism is not important for populating the (3, 3)

manifold. Based on the diabatic curves of figure 1, qualitatively, states in the (3, 3) and (3, 4) manifolds can be populated by a two-step mechanism as follows: in the first step, the $C^{5+}(n=3)$-He^{+} channel is populated at the crossing at $R=5$ au. The $C^{5+}(n=3)+He^{+}$ channel crosses with the (3, 3) manifold at smaller internuclear separations where the second electron in He^{+} is captured. On exit, the system separates following the (3, 3) diabatic curves. This two-step mechanism invokes a portion of relatively repulsive trajectories and thus the (3, 3) states are populated at large scattering angles, in agreement with the experimental data of Roncin *et al* (1989).

We next discuss the mechanism for populating the $(2, n=3\text{–}6)$ manifolds. These states cross the entrance channels at $R=2.5$, 3.3, 3.8 and 4.1 for $n=3$, 4, 5 and 6, respectively. These crossing radii are not too far from $R=5.1$ where single capture to $n=3$ occurs. Thus one may speculate that each of the crossings can contribute to the population of $(2, n)$ states. On the other hand, at such small values of R, the two-step mechanism is important in general. It is likely that both mechanisms contribute to the population of $(2, n)$ states, but their relative importance within a given theoretical framework can only be determined by actual calculations.

We further consider whether a one-step mechanism for double capture can be attributed to a correlated process. For low-energy collisions, in the absence of MO correlation diagrams, the one- or two-step process has been defined with respect to the diabatic correlation diagram such as in figures 1 and 5. If the doubly excited state is populated through a single crossing with the entrance channel, it is defined as a one-step process. If the doubly excited state is populated through two successive crossings, the mechanism has been defined as a two-step mechanism. Similarly, without a precise definition, a correlated process has been used to mean that a given transition is not possible if the interelectronic interaction is neglected (a more precise definition in terms of the molecular Hartree–Fock model is desirable). With such a definition, it is *incorrect* to state that double capture is not allowed in a one-step process if the electron–electron interaction is neglected. A simple proof of this result is given in the appendix.

Based on the above analysis, we summarize the interpretation of the population mechanisms of $(2, n)$ and (3, 3) doubly excited states in C^{6+}–He or O^{6+}–He collisions

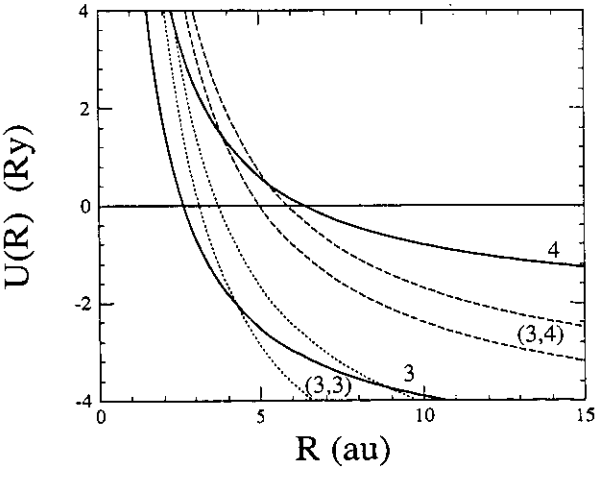

Figure 5. Schematic diabatic potential curves for O^{8+} + He system.

at low energies. From the diabatic potential curves of figure 1, the (3, 3) states cannot be populated by a one-step process between the (3, 3) states and the entrance channel. A two-step mechanism is needed through coupling of MO at small internuclear separations. For the population of $(2, n)$ $(n \geq 3)$ doubly excited states, one cannot rule out the contributions of both one-step and two-step processes since both occur at relatively small internuclear distances. We further argue that a one-step process based on the diabatic crossing between the entrance channel and the doubly excited state channel cannot be attributed to a correlated process in general.

3.2. $O^{8+}+He$

3.2.1. Total cross sections for double capture to 3l3l′ and 3l4l′ states. Double capture to the $3lnl'$ $(n \geq 3)$ manifolds has been studied by Mack *et al* (1989) for 96 keV $^{18}O^{8+}$ ions on He where the electron spectra were measured at 50°. The same system has also been studied by Moretto-Capelle *et al* (1989) at 80 keV where the electrons were measured at 10°. Both experiments were able to separate most of the individual doubly excited states of the $3l3l'$ manifold. The same system has also been investigated using energy gain spectroscopy by Roncin *et al* (1989) at a much lower energy of 10 keV where the angular distributions of the scattered projectiles were measured to obtain information about the internuclear distances where double capture occurs. However, the latter method did not separate individual doubly excited states formed, but the (3, 3) and (3, 4) manifolds were separated. This collision system has also been studied by Mann (1987) using electron spectroscopy and by Bliman *et al* (1983) by analysing the charge state of the projectiles. In the later experiment, $\sigma_{q,q-1}$ was measured. One can take $\sigma_{q,q-1}$ to be the sum of cross sections for single capture and double capture to doubly excited states since the latter decay almost exclusively by electron emission. At present, there still exist large discrepancies among experimental single and double capture cross sections, see the discussion in section 5 of Moretto-Capelle *et al* (1989).

On the theoretical side there exist two close coupling calculations based on expanding the two-electron wavefunctions in terms of molecular orbitals for the O^{8+}–He system. Because of the difficulty of including a large number of important single and double capture channels in the calculation, the basis set used in each calculation was severely truncated. In Bliman *et al* (1983), where a limited number of double capture channels were included, it was concluded that double capture cross sections are comparable to single capture cross sections. On the other hand, Kimura and Olson (1985) concluded that double capture was not important, but double capture channels were not included in their calculations. The importance of double capture has been established by Barat *et al* (1987) where the ratio of double capture to single capture cross sections was directly measured to be 0.29 at 10 keV. The same ratio at different energies has not been established yet.

In view of the difficulty of carrying out a complete two-electron calculation including all the important single and double capture channels, we applied the independent-electron model to this collision system. The diabatic correlation diagram for the present system is shown in figure 5. The crossing radii for single capture to $n=3$ and $n=4$ states are 2.6 and 6.4 au, respectively, and for double capture to the (3, 3) and (3, 4) manifolds are 3.2–3.7 and 5.0–5.9 au, respectively. Based on the correlation diagram and the differential scattering data of Laurent *et al* (1987) showing that the (3, 4) states are populated at much larger scattering angles than single capture to the $n=4$ states, we may argue that the (3, 4) manifold is formed in a two-step process where single

capture to the $n=4$ states occurs at $R \simeq 6$ for the first electron in the first step, with subsequent capture to the $n=3$ states for the second electron at smaller R in the second step. The data from Laurent *et al* (1987) showed that the (3, 3) states are populated at even larger scattering angles than the (3, 4) states. Thus the (3, 3) states are also populated through the two-step mechanism.

The impact parameter weighted probabilities for single electron capture to individual states in each of the two model calculations are shown in figure 6(*a*) and (*b*). In the first calculation, the $n=4$ states are populated mostly for b in the range of 3–7 au. The $n=3$ are populated only for b less than 3 au. In the second calculation for capture from He^+, the dominant capture is to the $n=3$ states in the range of impact parameters of 1.2–4 au. The products of these probabilities give an estimate of the range of b where (3, 3) and (3, 4) states are populated. it is clear that (3, 3) states are populated at smaller impact parameters than the (3, 4) states, consistent with the angular scattering data of Laurent *et al* (1987). The calculated cross sections for the collision energy at 96 keV for single capture to $n=3$ and $n=4$ states and double capture to (3, 3) and (3, 4) manifolds are summarized in table 3 where we also compare these results with other theories and experiments (at slightly different energies). We also compare the theoretical $\sigma_{q,q-1}$ which is taken as the sum of cross sections for single capture to $n=3$ and 4 states and double capture to (3, 3) and (3, 4) states, with the experimental values obtained from energy gain measurements. In table 3 we also show the cross sections for the population of (3, 3) and (3, 4) states and their ratio. The calculated cross sections agree reasonably with the data of Moretto-Cappelle *et al* (1989) where the cross sections were derived from electron measurements at 10° and the electron distribution was assumed to be isotropic. The calculated ratio is also compared with the result from the data of Barat *et al* (1987) at the lower energy of 10 keV. In figure 7 we show the total double capture cross sections to individual states within the (3, 3) manifold. Comparison of the calculation with the experimental Auger electron spectra at a particular angle will be discussed in the accompanying paper (Chen and Lin 1991).

From the double capture cross sections to individual doubly excited states, one can extract the relative population of 2s and 2p states of O^{7+} ions. Such information has been obtained experimentally by measuring the polarization of the Lyman radiation

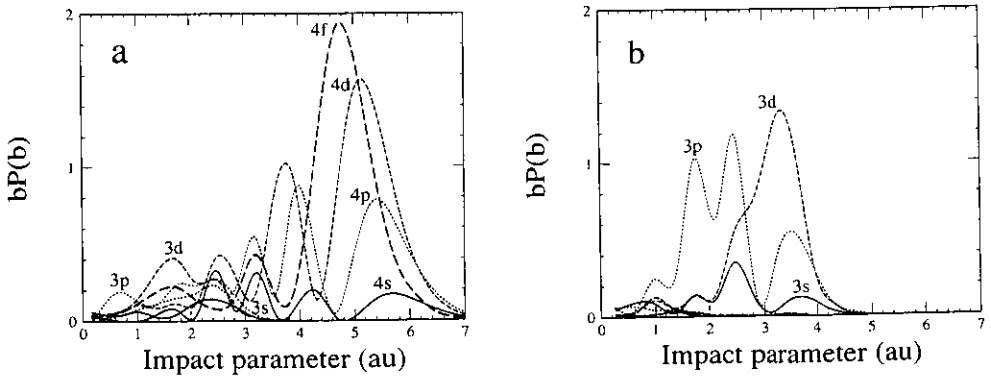

Figure 6. Impact parameter weighted probabilities for single capture to each *nl* state. (*a*) Single capture probabilities by O^{8+} from neutral He; (2) single capture probabilities by O^{8+} from He^+. The collision energy is 96 keV.

Table 3. Comparison of theoretical and experimental single (sc) and double (dc) capture cross sections, and cross sections $\sigma(3,3)$ and $\sigma(3,4)$, respectively, for double capture to the (3, 3) and (3, 4) manifolds for O^{8+} + He collisions. The cross sections are given in units of 10^{-16} cm^2. The theoretical results are from the present calculation at 96 keV. The experimental results are at different energies (see table).

	Theory	Experiment
single capture	16[a], 13[b]; 22[c]	
$\sigma(3,3)$	5.3[a], 1.8[b]	
$\sigma(3,4)$	9.3[a], 3.0[b]	
$\sigma(sc)+\sigma(dc)$	31[a], 18[b]	17 ± 3.4[b]; 23 ± 4.6[d]; 34.4 ± 6.9[e];
$\sigma(3,3)/\sigma(3,4)$	0.57[a], 0.60[b]	0.85[f]; 0.64[g]

[a] Present results.
[b] Bliman *et al* (1983).
[c] Kimura and Olson (1985).
[d] Afrosimov *et al* (1982).
[e] Iwai *et al* (1982) at 18 keV.
[f] Moretto-Capelle *et al* (1989) at 80 keV.
[g] Barat *et al* (1987) at 10 keV.

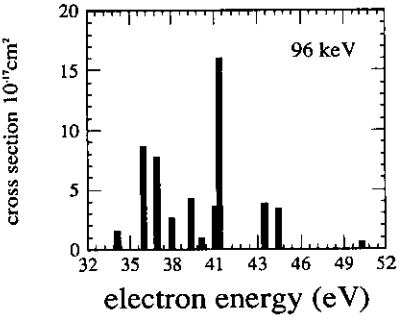

Figure 7. Calculated state selective double capture cross sections for $O^{8+}+He \Rightarrow O^{6+}(3l3l')+He^{2+}$ at 96 keV.

after the autoionization of doubly excited states in coincidence with the energy gain of the incident ion. The energy gain spectra can only resolve the $3l3l'$ and $3l4l'$ manifolds. The ratio of 2s relative to 2p, $R(2s/2p)$, of the O^{7+} ions measured by Touati *et al* (1987) at 10 keV ion energy is 0.6–4. From the relative double capture cross sections to individual doubly excited state we calculate the ratios $R(2s/2p)$ for the $3l3l'$ and the $3l4l'$ manifolds at 96 keV to be 0.26 and 0.27, respectively. The same ratio derived from the electron spectra of Moretto-Capelle *et al* (1989) at 80 keV for the $3l3l'$ manifold is 0.21–0.24. One possible reason for the discrepancy with the data of Touati *et al* (1987) is that their experiments were carried out at a much lower collision energy. In calculating the ratio, $R(2s/2p)$, we used the autoionization branching ratio calculated by Bachau (in Chetioui *et al* 1989). The small $R(2s/2p)$ from our calculation and from Moretto-Capelle *et al* (1989) implies that high-L doubly excited states are populated. This result is a reflection of the fact that high-l states are populated in the single capture process. The large population of high-L doubly excited states suggests that these states 'consist' of products of high-l singly excited states.

4. Summary

In this article we studied double capture to doubly excited states for the collisions of bare carbon and oxygen ions with helium atoms in the energy range of a few keV amu^{-1} using the independent-electron model. The capture process is approximated as a two-step process where the first electron is captured from the neutral He atom, while in the second step the electron is captured from the relaxed He^+ ion. The electron capture amplitudes to individual singly excited states are calculated using the two-centre close-coupling method expanded in terms of atomic orbitals. These amplitudes are then combined to form amplitudes for double capture to individual doubly excited states from which double capture cross sections are derived. The results are compared with cross sections calculated by other theories which do not assume an independent-electron model and with experiments. For C^{6+} on He, where double capture is only about 10% of the single capture cross section, we note that there is an overall agreement between the present calculation and the other theoretical and experimental cross sections for both single and double capture (see table 2). The situation is less obvious for O^{8+} on He where double capture is evaluated to be about 50–100% of single capture (see table 3). On the experimental side, there exist large discrepancies even for the total single and double capture cross sections. On the theoretical side, the close coupling calculations based on expanding the two-electron wavefunctions in terms of travelling molecular orbitals disagree substantially, most probably because of the severe truncation of the basis set adopted in each calculation. The present independent-electron model calculation, where 60–70 basis functions were used in each calculation, amounts to a much larger basis set in a two-electron calculation. On the other hand, we adopted an intuitive independent-particle approximation and obtained cross sections for both single and double capture in reasonable agreement with experiments. We conclude that the major features of double capture at low energies can be interpreted by the present independent-electron approximation. On the other hand, it is premature to assert the validity of the present model. It is desirable that the theoretical calculations should compare not only the single and double capture cross sections, but also the different subshell cross sections. For single capture processes, cross sections for different *nl* final states have been determined by following the photon emissions. For double capture to doubly excited states, it is desirable to make comparison with the electron emission cross sections from different states. This is addressed in the following paper (Chen and Lin 1991).

We also discussed the role of electron correlation for the population of doubly excited states. The general qualitative agreement between the present calculation and experiments indicates that electron correlation does not play any dominant role in the collision process. In other words, there are no distinct features in the double capture process where electron–electron interaction plays a major role. This is different from collisions at higher energies where there are special features that can be attributed to electron–electron interactions (see Fritsch and Lin 1988, 1990 and references therein).

Acknowledgment

This work is supported in part by the US Department of Energy, Office of Basic Energy Sciences, Division of Chemical Sciences. We thank Nico Stolterfoht for communicating his results prior to publications.

Appendix. Analysis of double capture processes in the independent-electron approximation

Consider the collision of a bare ion of nuclear charge Z with a helium atom in the independent-particle approximation. The Hamiltonian for the two-electron system can be written as

$$H = -\tfrac{1}{2}\nabla_1^2 - \tfrac{1}{2}\nabla_2^2 + V_t(r_1) + V_t(r_2) - \frac{Z}{r_{1p}} - \frac{Z}{r_{2p}}. \tag{A1}$$

Consider the curve crossing problem where only the incident channel and one final double capture channel are considered. The wavefunctions for the two diabatic states are $u_t(1)u_t(2)$ for the initial state, where both electrons are on the target, and $v_p(1)v_p(2)$ for the final state, where both electrons are on the projectile, respectively. The diabatic curves for these two channels cross at a certain internuclear separation. Our question is whether double capture can occur at the crossing within the independent-electron model as given by the Hamiltonian (A1). In the two-state approximation, the adiabatic molecular wavefunctions at each internuclear separation R are given by

$$\Psi_i(r_1, r_2, R) = a_i(R)u_t(1)u_t(2) + b_i(R)v_p(1)v_p(2) \tag{A2}$$

for $i = 1, 2$ where the coefficients $a_i(R)$ and $b_i(R)$ can be obtained by solving $(H - E)\Psi = 0$ at each R. In the adiabatic representation, the radial coupling term can be calculated according to

$$\langle \Psi_1 | \mathrm{d}/\mathrm{d}R | \Psi_2 \rangle = a_1(R)\frac{\mathrm{d}a_2(R)}{\mathrm{d}R} + b_1(R)\frac{\mathrm{d}b_2(R)}{\mathrm{d}R}. \tag{A3}$$

This term is non-zero in general and thus double capture can occur at the crossing. In this derivation the interelectronic interaction was not included in the Hamiltonian (A1). We conclude that it is incorrect to ascribe a one-step process for double capture entirely to electron–electron interaction.

The same conclusion can be drawn from another viewpoint. In a many-electron MO model, there are only radial and angular couplings. The interelectronic interaction will modify each coupling term, but the modification is a smooth function of the internuclear distance R. For example, it has often been asserted that double capture to the $C^{2+}(1s^2 2s^2)$ final state in $C^{4+} + He$ collisions at low energies is a manifestation of the importance of electron correlation. This state is populated as the result of the avoided crossing at $R = 3.0$ au (Kimura and Olson 1984). However the location of this avoided crossing is expected to only shift slightly if the electron–electron interaction term is replaced by a screened one-electron model potential. In the latter approximation, one can still obtain a non-zero double capture probability.

References

Afrosimov V V, Basalaev A A, Donets E D, Lozhkin K O and Panov M N 1982 *Proc. 12th Int. Conf. on Physics of Electronic and Atomic Collisions* (Amsterdam: North-Holland) p 690

Barat M, Gaboriaud M N, Guillemont L, Roncin P, Laurent H and Andriamonje S 1987 *J. Phys. B: At. Mol. Phys.* **20** 5771

Bliman S, Hitz D, Jacquot B, Harel C and Salin A 1983 *J. Phys. B: At. Mol. Phys.* **16** 2849

Bordenave-Montesquieu A, Benoit-Cattin P, Boudjema M, Gleizes A, Dousson S and Hitz D 1987 *Proc. 15th Int. Conf. on the Physics of Electronic and Atomic Collisions (Brighton, 1987)* ed J Geddes *et al* (Amsterdam: North-Holland) Abstracts p 551

Bordenave-Montesquieu A, Boudjema M, Benoit-Cattin P, Gleizes A and Moretto-Capelle P 1989 *J. Physique* C1 **50** 305

Boudjema M, Moretto-Capelle P, Bordenave-Montesquieu A, Benoit-Cattin P, Gleizes A, Bachau H, Martín F, Riera A and Yáñez M 1989 *J. Phys. B: At. Mol. Opt. Phys.* **22** L121

Chen Z and Lin C D 1991 *J. Phys. B: At. Mol. Opt. Phys.* **24**

Chetioui A, Bachau H, Wohrer K, Vernhet D, Blumenfeld L, Politis M F, Rozet J P, Touati A and Stephan C J 1989 *J. Phys. B: At. Mol. Opt. Phys.* **22** 2865

Dijkkamp D, Ciric D, Vlieg E, de Boer A and de Heer F J 1985 *J. Phys. B: At. Mol. Phys.* **18** 4763

Fritsch W and Lin C D 1986 *J. Phys. B: At. Mol. Phys.* **19** 2683

—— 1988 *Phys. Rev. Lett.* **61** 690

—— 1990 *Phys. Rev.* A **41** 4776

Harel C and Jouin H 1990 *Europhys. Lett.* **11** 121

Iwai T, Kaneko Y, Kimura M, Kobayashi N, Ohtani S, Okuno K, Takagi S, Tawara H and Tsurubuchi S 1982 *Phys. Rev.* A **26** 105

Jain A, Lin C D and Fritsch W 1989 *Phys. Rev.* A **39** 1741

Kimura M and Olson R 1984 *J. Phys. B: At. Mol. Phys.* **17** L713

—— 1985 *J. Phys. B: At. Mol. Phys.* **18** 2729

Kimura M, Sato H and Olson R E 1983 *Phys. Rev.* A **28** 2085

Laurent H, Barat M, Gaboriaud M N, Guillemot L and Roncin P 1987 *J. Phys. B: At. Mol. Phys.* **20** 6581

Lin C D 1986 *Adv. At. Mol. Phys.* **22** 76

—— 1989 *Phys. Rev.* A **39** 4355

Liu C J, Dunford R W, Berry H G, Pardo R C, Groeneceld K O, Hass M and Raphaelian M L A 1989 *J. Phys. B: At. Mol. Opt. Phys.* **22** 1217

Mack M, Nijland J H, van der Straten P, Niehaus A and Morgenstern R 1989 *Phys. Rev.* A **39** 3846

Mann R 1987 *Phys. Rev.* A **35** 4988

Moretto-Capelle P, Oza D H, Benoit-Cattin P, Bordenave-Montesquieu A, Boudjema M, Gleizes A, Dousson S and Hitz D 1989 *J. Phys. B: At. Mol. Opt. Phys.* **22** 271

Niehaus A 1986 *J. Phys. B: At. Mol. Phys.* **19** 2925

Roncin P, Barat M, Gaboriaud M N, Guillemot L and Laurent H 1989 *J. Phys. B: At. Mol. Opt. Phys.* **22** 509

Sakaue H A *et al* 1989 *Proc. 16th Int. Conf. on the Physics of Electronic and Atomic Collisions (New York, 1989)* A Dalgarno *et al* (Amsterdam: North-Holland) Abstracts p 570

—— 1990 *J. Phys. B: At. Mol. Opt. Phys.* **23** L401

Shimakura N, Sato H, Kimura M and Watanabe T 1987 *J. Phys. B: At. Mol. Phys.* **20** 1801

Shingal R 1988 *J. Phys. B: At. Mol. Opt. Phys.* **21** 2065

Stolterfoht N, Havener C C, Phaneuf R A, Swenson J K, Shafroth S M and Meyer F W 1986 *Phys. Rev. Lett.* **57** 74

Stolterfoht N, Sommer K, Swenson J K, Havener C C and Meyer F W 1990 *Phys. Rev.* A **42** 5396

Touati A, Chetioui A, Wohrer K, Rozet J P, Politis M F, Vernhet D, Blumenfeld L, Roncin P, Gaboriaud M N, Barat M, Dousson S and Hitz D 1987 *Nucl. Instrum. Methods* B **23** 64

Zouros T J M, Schneider D and Stolterfoht N 1987 *Phys. Rev.* A **35** 1963